

# Isothermal devitrification of an oxynitride LAS glass composition monitored by X-ray powder diffraction

JEAN ROCHERULLÉ

UMR CNRS 6512 Verres et Céramiques, Institut de Chimie de Rennes, Université de Rennes I, Avenue du Général Leclerc, 35042 Rennes cedex, France  
E-mail: jean.rocherulle@univ-rennes1.fr

The crystallisation of a  $\text{Li}_{0.6}\text{Al}_{0.1}\text{Si}_{0.6}\text{O}_{1.575}\text{N}_{0.05}$  glass matrix has been studied by means of X-ray powder diffraction at  $730^\circ\text{C}$ . Data diffraction and EDS analysis have shown the simultaneous formation of two crystalline phases  $\text{Li}_2\text{SiO}_3$  and  $\text{Li}_{0.6}\text{Al}_{0.6}\text{Si}_{2.4}\text{O}_6$  (so-called virgilite) with no evidence for the presence of nitrogen in these phases. The Avrami exponent has been determined for each phase from several time-dependent X-ray diffraction studies. The values of the Avrami exponent, close to 2.25, suggest that crystallisation is tri-dimensional and controlled by a diffusion process with a decreasing nucleation rate at  $730^\circ\text{C}$ . With respect to the aluminium-containing phase, a long time heat treatment at this temperature has not revealed a phase transition from the metastable hexagonal symmetry to the stable tetragonal one. The XRD correlation length values, from the Scherrer equation, are close to 450 Å. Furthermore, SEM micrographs have confirmed the volume crystallization of this glass composition and the approximate linear dimension of the regions of diffracting materials. © 2003 Kluwer Academic Publishers

## 1. Introduction

Structural transformations like glass crystallisation affect materials stiffness and generally enhance the mechanical characteristics of the materials. Likewise, it is well known that partial replacement of oxygen by nitrogen in a lithium containing aluminosilicate glass increases hardness, viscosity, glass transition temperature and elastic moduli [1]. In addition, the subsequent crystallization of oxynitride glass ceramics has been shown to further enhance the properties of these materials [2]. Differential Scanning Calorimetry (DSC) and Differential Thermal Analysis (DTA) are the usual and convenient means of investigations for this first order phase transformation involving both nucleation and growth. Different analytical methods have been developed and studies can be performed from isothermal or non-isothermal experiments. Nevertheless, when the temperature range for crystallisation is located beyond  $600^\circ\text{C}$ , only non-isothermal studies are well suited.

Concerning the solid-state transformations occurring in crystalline materials, extensive investigations based on neutron powder diffraction or X-ray diffraction using synchrotron radiations have been reported in the literature [3–6]. Despite the lower intensity obtained with a conventional X-ray source, the use of powder diffraction in laboratory has become a relevant tool for the characterisation of structural or microstructural changes in materials [7]. Nevertheless, no systematic investigations on the devitrification phenomenon studied from this way have been undertaken previ-

ously, except for the study of a phase transformation in  $\text{SrAl}_2\text{Si}_2\text{O}_8$  glass [8]. In this specific field, the temperature and time-dependent X-ray diffraction could be viewed as a most valuable technique that completes more conventional methods such as DSC or DTA [9].

Consequently, the aim of this paper is to study, from a time-dependent X-ray diffraction analysis, the crystallization behaviour of an oxynitride glass composition described by  $\text{Li}_{0.6}\text{Al}_{0.1}\text{Si}_{0.6}\text{O}_{1.575}\text{N}_{0.05}$ . This can be useful for the designing of glass ceramic in order to combine strength, toughness and the potential for high temperature oxidation resistance.

## 2. Analytical method

The Avrami's law applies well to isothermal devitrification studies of glasses [10]. This law may be written as:

$$x = 1 - \exp[-kt^n] \quad (1)$$

where  $x$  is the volume fraction crystallised after time  $t$ ,  $n$  is the Avrami's exponent and  $k$  is defined as the apparent reaction rate, which is usually assigned an Arrhenian temperature dependence:

$$k = k_0 \exp(-E/RT) \quad (2)$$

where  $E$  is the activation energy describing the overall crystallisation process.

After rearrangement of Equation 1, one obtains:

$$\ln[-\ln(1-x)] = \ln k + n \ln t \quad (3)$$

Relation (3) gives directly the values of  $n$  by plotting  $\ln[-\ln(1-x)]$  versus  $\ln t$ .

Consequently, the Avrami exponent can be determined from experimental values of the crystallized volume fraction. Theoretically, the  $x$  value at a time  $t$  can be obtained from  $I(hkl)$ , the diffracted intensity of  $hkl$  reflections at the same time.  $I(hkl)$  is given by the well-known equation:

$$I(hkl) = mL^2 F^2(hkl) V p(hkl) \quad (4)$$

where  $m$  is the multiplicity factor,  $L$  the Lorentz-polarisation factor,  $F(hkl)$  the structure factor for a reflection  $hkl$ ,  $V$  the effective diffracting volume of the sample and  $p$  the preferred orientation factor for the reflection  $hkl$ . In principle, the  $p$  factor value should be constant during the transformation. In practice, over one independent diffraction line is considered in the analysis. In addition, to avoid dramatic changes in diffraction lines intensities leading to subsequent abnormal variation of the transformed volume fractions, a careful preparation of the starting powder is needed by checking that the crystallites are randomly oriented in the sample. Nevertheless, if the  $x$  value for the quenched glass sample can be obviously estimated to zero, we must take care to the determination of  $x$  value for an infinite heating time ( $x_\infty$ ). The devitrification is never complete, it always remains a residual glassy phase which is not a diffracting material. However, the corresponding volume fraction could be estimated from background measurements to be less than a few per cent. Thus, the  $x$  value will be considered as 1.0 and the volume fraction expected to be crystallized at time  $t$  will be defined by the ratio (Equation 5) of the integrated intensity of a diffraction line at time  $t$  over the maximum of the integrated intensity reached by the same diffraction line:

$$x_t = \frac{I(hkl)_t}{I(hkl)_\infty} \quad (5)$$

### 3. Experimental

#### 3.1. Glass synthesis and thermal treatment

Starting materials were commercial products  $\text{Al}_2\text{O}_3$  (Johnson Matthey)  $\text{SiO}_2$  (Quartz et Silice) and  $\text{Li}_2\text{SiO}_3$  (Aldrich). A single piece of glass ( $\approx 50$  g) has been prepared by melting up to  $1300^\circ\text{C}$  the powders inside of a molybdenum crucible under a nitrogen atmosphere to prevent oxidation. Then, the melt has been poured into a molybdenum mould at room temperature. In this work, the overall crystallisation process of the quenched glass was not influenced by the impurity content of the starting materials (less than 0.5%). Some physical characteristics of this glass composition (from Ref. [1]) are summarized in Table I.

All the glass samples used in these isothermal studies were bulk specimens (weight:  $500 \text{ mg} \pm 10 \text{ mg}$ ) from the single piece of glass. The isothermal study was performed at  $730^\circ\text{C}$  during various times. Temperature was measured by means of a chromel-alumel

TABLE I Physical characteristics of the quenched glass

N content (atomic %)	$\rho$ ( $\text{g}\cdot\text{cm}^{-3}$ )	$E$ (GPa)	$\alpha \cdot 10^7$ ( $^\circ\text{C}^{-1}$ )	$\nu$	$Hv$ (MPa)	$T_g$ ( $^\circ\text{C}$ )
3.07	2.42	90	105	0.23	5100	500

Experimental density ( $\rho$ ), Young modulus ( $E$ ), Thermal expansion coefficient ( $\alpha$ ), Poisson's ratio ( $\nu$ ), Vickers microhardness ( $Hv$ ), Glass transition at 10 K/min ( $T_g$ ).

thermocouple in contact with the bulk sample inside an inert platinum crucible. The temperature of the bulk sample can be considered as homogeneous after one minute at the working temperature, so we can assume that no crystallisation occurs during this short time.

#### 3.2. X-ray diffraction analysis

The crystalline phases obtained after the heat treatment were identified by X-ray powder diffraction. Data were collected with a PHILIPS diffractometer, using  $\text{Cu K}\alpha$  radiation [ $\lambda(K\alpha_1) = 1.5406 \text{ \AA}$ ,  $\lambda(K\alpha_2) = 1.5444 \text{ \AA}$ ] and the Bragg Brentano optics. Phases were identified by interrogation of the ICDD PDF-2 database incorporated in the program SEARCH/MATCH available in the PC software package X'PERT supplied by Philips. In order to minimise the diffraction lines broadening, the heated bulk samples were grounded and sifted to select a single granulometry class in the range from 20 to  $50 \mu\text{m}$ . As the diffraction line intensity is a function of the crystallized volume fraction, the weight of the analyzed powder samples must remain the same. Because of the relatively slow rate of the devitrification, short heating times yield to particularly low  $x$  values. Then, in this slow transformation, high quality data were required and were collected *ex situ* with a scintillator detector. Finally, to ensure satisfactory counting statistics, the diffraction patterns were scanned with a step length of  $0.04^\circ$  ( $2\theta$ ) and a counting time of  $20 \text{ s} \cdot \text{step}^{-1}$ . Integrated intensities were extracted from selected diffraction lines by using the program PROFIT supplied by Philips.

### 4. Results and discussion

#### 4.1. Phase identification

The presence of several components in the glass provides a possibility of forming a large number of crystalline species. Moreover, the nature of the crystalline phases is mainly influenced by the heat treatment and the grain size of the initial specimens. Thus, the different phases that were present in the bulk samples after the isothermal experiment have been clearly identified. Fig. 1 represents a typical XRD pattern obtained for a glass sample previously heated up to  $800^\circ\text{C}$  in the DTA apparatus and then cooled down to room temperature.

The diffraction patterns show the simultaneous presence of  $\text{Li}_2\text{SiO}_3$  (PDF2 file No. 29-0828) and another phase identified as  $\text{Li}_{0.6}\text{Al}_{0.6}\text{Si}_{2.4}\text{O}_6$  (PDF 2 file No. 31-0707), a mineral so called virgilite with a hexagonal symmetry. Until now, this last has been only observed in a volcanic glass of unusual composition from

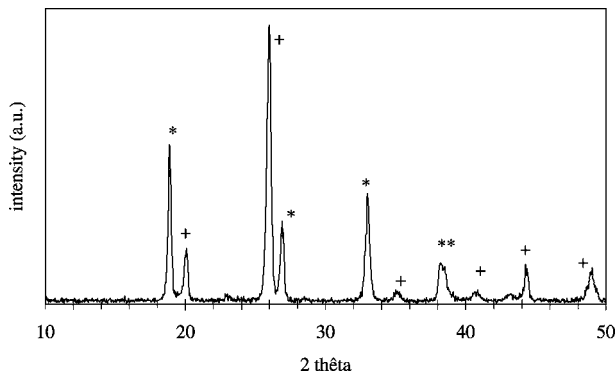


Figure 1 Phase identification (\*)  $\text{Li}_2\text{SiO}_3$  (+)  $\text{Li}_{0.6}\text{Al}_{0.6}\text{Si}_{2.4}\text{O}_6$ .

Macusani, Peru [11]. This mineral is the only known naturally occurring member of the  $\beta$ -quartz solid solution between  $\text{LiAlSi}_2\text{O}_6$  and  $\text{SiO}_2$ . In addition, an EDS analysis has confirmed there was no evidence for the presence of nitrogen in the different crystalline phases. Besides, a long time heat treatment at  $730^\circ\text{C}$  has not revealed a phase transition from the hexagonal symmetry to the tetragonal one (PDF 2 file No. 21-503) for the aluminium-containing phase. This was mentioned in a previous study performed on a pure oxide glass with the same cationic composition [12].

#### 4.2. Isothermal study at $730^\circ\text{C}$

Fig. 2 represents the crystallized volume fraction at  $730^\circ\text{C}$  as a function of time logarithm, for both the silicate (LS) and aluminosilicate (LAS) phases. The  $x$  values have been determined from several diffraction lines. With regard to the time dependence, there is no difference between the two crystalline phases and the devitrification can be considered as achieved after 90 min. Collected patterns have revealed an important diffraction line broadening especially for short heating time, but no preferred orientation effect were present as shown in Fig. 3a and b. Regarding the time dependence, the LS and LAS crystallized volume fractions obtained from different diffraction lines do not exhibit any difference.

Fig. 4a and b show the plot of  $\text{Ln}(-\text{Ln}(1-x))$  versus  $\text{Ln}(t)$ , at  $730^\circ\text{C}$ , for the LS and LAS phases, respectively. After least-squares treatments, the slopes of these straight lines allow the determination of the

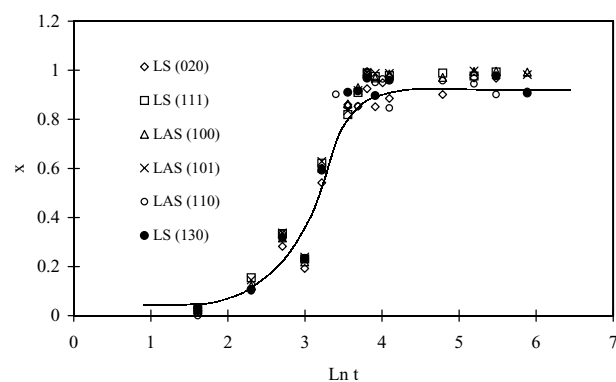
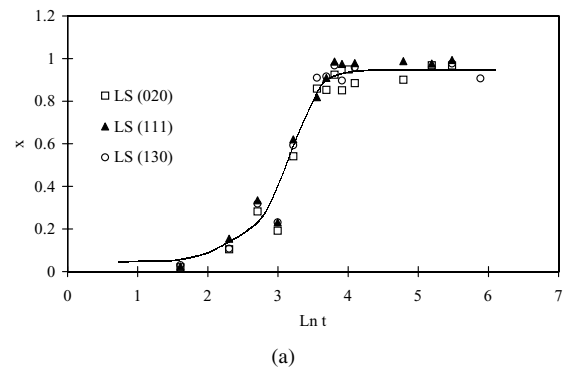
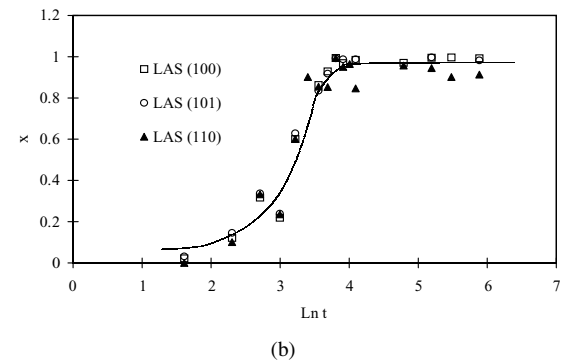


Figure 2 Crystallized volume fraction for both the LS and LAS phases as a function of time logarithm.

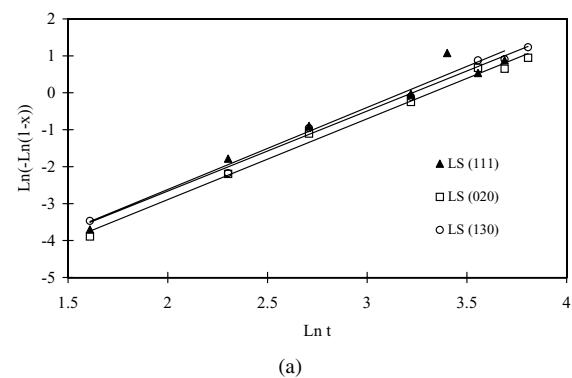


(a)

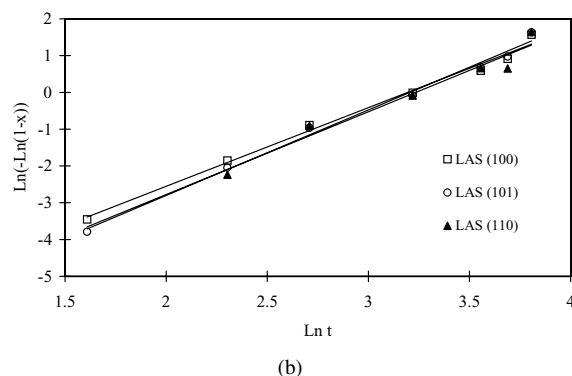


(b)

Figure 3 (a) Crystallized volume fraction as a function of time logarithm from diffraction lines of the LS phase. (b) Crystallized volume fraction as a function of time logarithm from diffraction lines of the LAS phase.



(a)



(b)

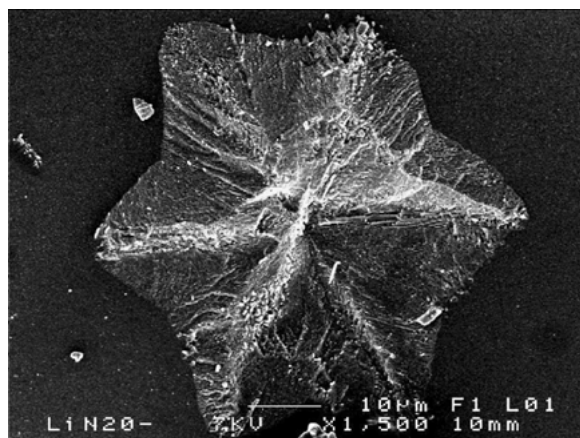
Figure 4 (a) Determination of the Avrami exponent from diffraction lines of the LS phase. (b) Determination of the Avrami exponent from diffraction lines of the LAS phase.

Avrami exponent. Table II summarizes the different values obtained from the LS powder diffraction data of three diffraction lines [(020), (111) and (130)] with the respective relative intensities 100%, 65% and 65%. There is a slight discrepancy between the calculated  $n$  values (from 2.18 to 2.22). Likewise, Table II gives this

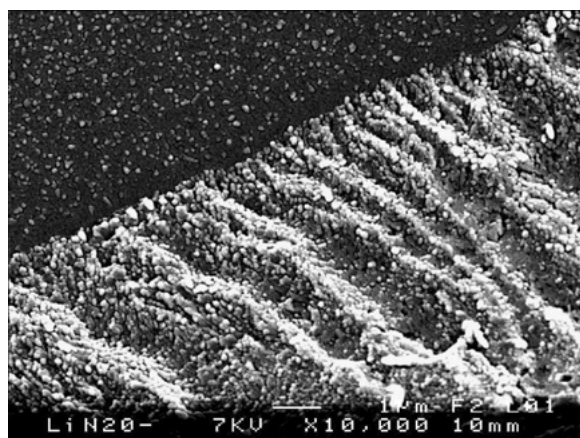
TABLE II Determination of the Avrami exponent from data diffraction of the LS and LAS phases

Crystalline phase	Diffraction line	Relative intensity	$n \pm \Delta$	$\langle n \rangle$
Li <sub>2</sub> SiO <sub>3</sub>	(020)	100	2.22 ± 0.04	2.21
	(111)	65	2.22 ± 0.09	
	(130)	65	2.18 ± 0.04	
Li <sub>0.6</sub> Al <sub>0.6</sub> Si <sub>2.4</sub> O <sub>6</sub>	(100)	13	2.14 ± 0.05	2.24
	(101)	100	2.33 ± 0.05	
	(110)	6	2.25 ± 0.13	

parameter determined from the LAS powder diffraction data. Three diffraction lines have also been selected, (101), (100) and (110), with the corresponding relative intensities 100%, 13% and 6%. The corresponding values found for the Avrami exponent corroborate the previous result relating to the growth of the LS phase. Considering the glass devitrification, the growing of the two crystalline phases is simultaneous. Furthermore, in accordance with a previous work performed by Christian [13], the values of the Avrami exponent are also indicative of a tri-dimensional crystallisation controlled by a diffusion process with a decreasing nucleation rate at 730°C. In addition, several SEM micrographs of a bulk glass (JEOL field emission SEM model JSM 6301F), crystallized at 730°C during 20 minutes, have been done. Fig. 5a shows, inside of



(a)



(b)

Figure 5 (a) SEM micrograph of a crystallized grain in the bulk sample showing the general feature of internal crystallization. (b) SEM micrograph of the interface between the grain and the residual glassy phase.

the bulk sample, a typical grain with a hexagonal shape. The size of this grain is close to 60 μm. Besides, Fig. 5b shows, at a higher magnitude, the interface between this grain and what is considered as the residual glassy phase. As one can see, the so-called glassy phase reveals the presence of small particles, with an approaching size value of 600 Å. These particles seem to move in the direction of the grain in order to enhance its size. Moreover, assuming the Scherrer equation, the correlation length can be linked to diffraction line profile by:

$$D = \frac{k\lambda}{\beta \cos \theta} \quad (6)$$

where  $D$  is a linear dimension in Å,  $k$  is a constant ( $\sim 0.9$ ),  $\lambda$  is the wavelength of the scattering radiation,  $\beta$  is the half-width of the diffraction line (in radians) and  $\theta$  is the Bragg angle. Typical values for  $D$ , from different integrated intensities, are close to 450 Å. These values have the same order of magnitude than those ones determined for the crystallite size from SEM data. Consequently, it can be assumed that the small particles shown in Fig. 5b are regions of typical coherently diffracting materials.

## 5. Conclusion

This study of a Li<sub>0.6</sub>Al<sub>0.1</sub>Si<sub>0.6</sub>O<sub>1.575</sub>N<sub>0.05</sub> glass crystallisation has shown that X-ray powder diffraction can be considered as a relevant tool for the determination of the kinetic parameters of the Avrami's law applied to this first order phase transformation. Confronted to DTA experiments, XRD can lead to a better understanding of the phenomenon and sheds light on the limits of thermal analysis in regard to glass devitrification involving nucleation and growth of several different crystalline phases. Furthermore, XRD should be able to supply a lot of information about all the structural and microstructural changes by studying the diffraction line profile. In this way, XRD experiments have allowed to consider the small crystallites observed in SEM micrographs as regions of coherently diffracting materials.

## References

1. J. ROCHERULLÉ, J. GUYADER, P. VERDIER and Y. LAURENT, *J. Mater. Sci.* **24** (1989) 5733.
2. A. NORDMANN and YI-BING CHENG, *J. Amer. Ceram. Soc.* **80**(12) (1997) 3045.
3. J. PANNETIER, *Chemica Scripta* **26A** (1986) 131.
4. O. SÄVBORG, J. R. SCHOONOVER, S. H. LIN and L. EYRING, *J. Solid State Chem.* **68** (1987) 214.
5. V. KOLARIK, M. JUEZ-LORENZO, N. EISENREICH and W. ENGEL, *Journal de Physique IV C9* (1993) 447.
6. O. ISNARD, J. L. SOUBEYROUX, S. MIRAGLIA, D. FRUCHART, L. M. GARCIA and J. BARTOLOME, *J. Physica* **180/181B** (1992) 624.
7. P. BÉNARD, J. P. AUFFREDIC and D. LOÛER, *Materials Sciences Forum* **228-231** (1996) 325.
8. C. H. DRUMMOND and N. P. BANSAL, *Bol. Soc. Esp. Ceram. Vid.* **31-C(2)** (1992) 41.
9. J. PLÉVERT, J. P. AUFFREDIC, M. Louër and D. Louër, *J. Mater. Sci.* **24** (1989) 1913.

10. J. ROCHERULLÉ and T. MARCHAND, *Mat. Res. Bull.* **35** (2000) 9.
11. B. M. FRENCH, P. A. JEZEK and D. E. APPLEMAN, *Am. Miner.* **63** (1978) 461.
12. J. ROCHERULLÉ and P. BÉNARD-ROCHERULLÉ, *Solid State Sciences* **4** (2002) 999.

13. J. W. CHRISTIAN, "The Theory of Transformations in Metals and Alloys," 2nd ed. (Pergamon, New York, 1971).

*Received 22 May  
and accepted 16 October 2002*